

High-speed Wireline Communication Systems

Ian C. Wong, Daifeng Wang, and Brian L. Evans
Embedded Signal Processing Laboratory
The University of Texas at Austin

May 31, 2005

Abstract

This report is a literature survey on multicarrier wireline communication systems, focusing primarily on the recent enhancements to the physical layer in Discrete Multitone (DMT) Modulation systems. We investigate methods used to improve the data rate versus reach performance of DMT systems proposed in the G.992.3 Asymmetric Digital Subscriber Lines-2 (ADSL2) and G.992.5 ADSL2+ standards. We also explore multi-channel DMT techniques to further increase the data rates, which include loop bonding, spectrum balancing, and vectored-DMT.

Contents

1	ADSL2 and ADSL2+	3
1.1	Overview	3
1.2	Improved Modulation Efficiency	4
1.3	Reduced Framing Overhead	4
1.4	Higher Coding Gain	5
1.5	Improved Initialization	5
1.5.1	Power Cutback	5
1.5.2	Spectral Shaping	8
1.5.3	Receiver-determined pilot tones	9
1.6	On-line Reconfiguration	11
1.6.1	Bit Swapping	11
1.6.2	Dynamic Rate Repartitioning	12
1.6.3	Seamless Rate Adaptation	12
1.6.4	On-line reconfiguration procedure	12
1.7	ADSL2+	13
2	Multichannel DMT	13
2.1	Loop Bonding	15
2.2	Spectrum Balancing	17
2.2.1	Single-line Power Control	18
2.2.2	Multi-line Power Control	19
2.2.3	Iterative Waterfilling	20
2.2.4	Optimal spectrum management	21
2.3	Vectored-DMT	24
2.3.1	Upstream: Successive interference cancelation	26
2.3.2	Downstream: MIMO Precoding	27
2.4	Initialization	27
2.4.1	Training Sequences	27
2.4.2	Channel Model	28
3	Preliminary Design Recommendations	29
3.1	Multichannel Technique Recommendations	29
3.2	Initialization Recommendations	30

1 ADSL2 and ADSL2+

In this section, we discuss the data rate versus reach improvements included in the G.992.3 ADSL2 standard [1]. A brief review of the improvements in G.992.5 ADSL2+ [2] is also included for completeness.

1.1 Overview

In July 2002, the ADSL2 standards G.992.3 and G.992.4 were published by the ITU [3]. These new standards address the problems service providers and subscribers faced in the original ADSL standard. The main improvements in ADSL2 versus ADSL are

1. Increased data rate versus reach
2. Improved loop diagnostics
3. Supported deployment from remote cabinets
4. Incorporated spectrum and power control
5. Increased robustness against loop impairments
6. Improved operations and maintenance mechanisms

We shall focus mainly on the first main improvement, which is the data rate versus reach performance.

The data rate improvements in ADSL2 were developed primarily for the case where the copper lines are long, and narrowband interference is predominant. This is the most challenging case for ADSL, since the main drawback in ADSL is its inability to serve reliably the customers that are situated far away from the central office. ADSL2 mandates a minimum of 8 Mbps downstream and 800 kbps upstream data rates, but typically achieves 12 Mbps and 1 Mbps upstream. This is accomplished through

1. Improved modulation efficiency
2. Reduced framing overhead
3. Higher coding gain
4. Improved initialization
5. Online reconfiguration

The following subsections shall discuss each of these in turn.

1.2 Improved Modulation Efficiency

ADSL2 provides higher modulation efficiency by mandating the block processing of Wei's [4] 16-state 4-dimensional trellis code [1, Ch. 8.6.2]. Data bits from the data frame buffer are first extracted according to the bit allocation table. These bits are then mapped into two binary words using the trellis encoder. An algorithmic constellation encoder is used to construct constellations with a maximum number of bits equal to the predefined maximum number of bits that each subcarrier can carry (8-15).

Aside from trellis coding, the optional mode of modulating data on the pilot tone is also used to improve modulation efficiency [1, Ch. 8.8.1.2] (The pilot tone is on subchannel 64, which is in the downstream group). During the initialization stage, the remote terminal receiver can set a bit to tell the central office transmitter that it wants to use the pilot tone for data. The transmitter will then treat the pilot tone just as any other data subcarrier in the DMT symbol. Although the improvement in data rate at first seems to be minimal using this enhancement, if we consider long lines where the data rates are around a few hundred kbps, adding, e.g. 8 extra bits in the pilot tone may give us an additional $8 \times 4 \text{ kHz} = 32 \text{ kbps}$, which may be significant in certain circumstances.

The third modulation efficiency improvement used in ADSL2 is the mandatory support for one-bit constellations [1, Ch. 8.6.3.2]. The constellation point of +1,+1 would signify a zero, and a point of -1,-1 would signify a one. With trellis coding, 2 1-bit constellations can be combined to build the 2-bit constellation generated by the trellis encoder. This improvement is also primarily useful for long lines, where at least one bit can be carried even for subcarriers with very low signal to noise ratios.

1.3 Reduced Framing Overhead

Unlike ADSL where overhead bits per frame are fixed and consume 32 kbps of actual payload data, ADSL2 allows a programmable framing overhead [1, Ch. 7.6]. This framing overhead can be varied between 4-32 kbps. This improvement can be significant particularly for long lines. For example, if the raw data rate is 128 kbps,

- For ADSL, we have $32/128=25\%$ overhead
- For ADSL2, we have $4/128=3.125\%$ overhead

Table 1: Initialization timing diagram.

Handshake procedures (G.994.1)	Channel discovery	Transceiver training	Channel analysis	Exchange
-----------------------------------	----------------------	-------------------------	---------------------	----------

1.4 Higher Coding Gain

In order to improve the performance of long lines, ADSL2 achieves a higher coding gain from the Reed-Solomon (RS) code [1, Ch. 7.7.1.4]. The flexible framing allows the RS code to have 0-16 redundancy octets in steps of 2. If the line is short and the signal to noise ratio is high, a small number of redundancy octets can be used to decrease the coding overhead. On the other hand, for poorer channels, higher coding gain can be achieved by using more redundancy octets.

1.5 Improved Initialization

ADSL transceiver initialization is required in order for a physically connected ATU-R and ATU-C pair to establish a communications link. Table 1 provides an overview of the initialization.

G.994.1, recommended by ITU-T, has two data frames: Capabilities List (CL) and Capabilities List Request (CLR). G.994.1 is a standard of handshake procedures for digital subscriber line (DSL) transceivers. It delivers some parameters required by ADSL2 standards as G.992.3 through certain data structures.

1.5.1 Power Cutback

Power cutback is the first main improved technology to reduce crosstalk and near-end echoes in ADSL2 initialization. Power allocated on upstream subcarriers can be moved to lower frequencies to avoid crosstalk. Improved transmit power cutback possibilities at both central office (CO) and remote side depend on the loop and local capabilities. Power cutback is the reduction of the transmit power spectrum density (PSD) level (expressed in dB) in any one direction, relative to the nominal transmit PSD level (NOMPSD). The same transmit PSD level reduction is applied over the entire frequency band (i.e., flat cutback).

NOMPSD is used at the start of initialization and relative to which subsequent transmit PSD level changes may occur, as determined by the transceivers during initialization and showtime. The showtime is the state of either ATU-C or ATU-R, reached after all initialization and training is

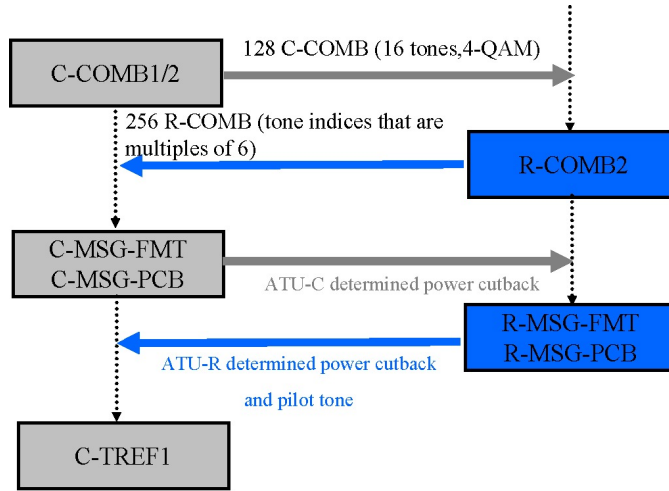


Figure 1: Timing diagram of Power cutback

completed, in which frame bearing data is transmitted. After power cutback in any one direction, NOMPSD becomes the reference transmit PSD level (REFPSD).

CL or CLR has a parameter block indicating the Nominal transmit PSD level, the Maximum transmit PSD level and the Maximum aggregate transmit power. The parameter block length shall be 6 bytes. These parameters shall be represented as a 9-bit 2's complement signed value in 0.1 dB steps, -25.6 to +25.5 dB. ATU-C estimates the minimum upstream or downstream power cutback for ATU-R during C-COMB1 and C-COMB2 states. ATU-R does it for ATU-C during R-COMB2.

Both ATU-C and ATU-R have the state in their initializations called C-MSG-PCB and R-MSG-PCB, respectively. C means the central office, i.e. ATU-C. R means the remote terminal, i.e. ATU-R. MSG indicates the message. PCB is short for Power Cutback. The state will convey the determined power cutback value stored in their transmitted MSG-PCB messages. The spectrum shaping on subcarriers, which will be described in next section, should be taken into account when determining the required upstream power cutback value. The timing diagram of power cutback is shown in Fig. 1 The data structures of C-MSG-PCB and R-MSG-PCB are shown in Fig. 2 and Fig. 3, respectively.

Bit index	Parameter	Definition
5...0	C-MIN_PCB_DS	ATU-C Minimum Downstream Power Cutback (6 bit value with MSB in bit 5 and LSB in bit 0)
11...6	C-MIN_PCB_US	ATU-C Minimum Upstream Power Cutback (6 bit value with MSB in bit 11 and LSB in bit 6)
13...12	HOOK_STATUS	Hook Status (2 bit value with MSB in bit 13 and LSB in bit 12)
15...14		Reserved, set to 0.
15 + <i>NSC_{us}</i> ...16	C-BLACKOUT	Blackout indication per subcarrier (subcarrier <i>NSC_{us}</i> – 1 in bit 15 + <i>NSC_{us}</i> , subcarrier 0 in bit 16). Bit 16 shall be set to 0 (i.e., no blackout of DC subcarrier).

Figure 2: C-MSG-PCB

Bit index	Parameter	Definition
5...0	R-MIN_PCB_DS	ATU-R Minimum Downstream Power Cutback (6 bit value with MSB in bit 5 and LSB in bit 0)
11...6	R-MIN_PCB_US	ATU-R Minimum Upstream Power Cutback (6 bit value with MSB in bit 11 and LSB in bit 6)
13...12	HOOK_STATUS	Hook Status (2 bit value with MSB in bit 13 and LSB in bit 12)
15...14		Reserved, set to 0
23...16	C-PILOT	Subcarrier index of downstream pilot tone (8 bit value with MSB in bit 23 and LSB in bit 16)
31...24		Reserved, set to 0
31 + <i>NSC_{ds}</i> ...32	R-BLACKOUT	Blackout indication per subcarrier (subcarrier <i>NSC_{ds}</i> – 1 in bit 31 + <i>NSC_{ds}</i> , subcarrier 0 in bit 32). Bit 32 shall be set to 0 (i.e., no blackout of DC subcarrier).

Figure 3: R-MSG-PCB

1.5.2 Spectral Shaping

The general shape of the DSL channel is such that higher frequencies are generally attenuated more than lower frequencies. ADSL systems allocate higher frequencies to the downstream. To improve the performance of ADSL on long loops, it is typically necessary to improve the downstream data rate. The upstream power can be moved lower in frequency to avoid crosstalk.

Based on DMT modulation, ADSL2 has some flexibility in shaping its transmit spectrum. Putting power where the channel is better (either by shrinking the range of the downstream frequencies or boosting the power) can improve the performance of ADSL2.

CL and CLR also have some required spectral shaping parameters. They have a parameter block of pairs of a subcarrier index and the spectrum shaping \log_tss_i value at that subcarrier. Pairs shall be transmitted in ascending subcarrier index order. Each pair shall be represented as 4 octets. The parameter block length shall be a multiple of 4 octets.

There is one bit in the parameter block indicating whether the subcarrier is included in the SUPPORTEDset (indication set to 1) or not included in the SUPPORTEDset (indication set to 0). SUPPORTEDset is defined by G.994.1 showing which subcarriers can be used. The spectrum shaping \log_tss_i values shall be represented in logarithmic scale as a 7-bit unsigned value in 0.5 dB steps, ranging from 0 dB (value 0) to 62.5 dB (value 125). Value 127 is a special value, indicating the subcarrier is not transmitted (i.e., $tss_i = 0$ in linear scale). Value 126 is a special value indicating that the \log_tss_i value on this subcarrier shall be linear interpolated according to the following diagram shown in Fig. 4.

Only four breakpoints are included in the CL/CLR message (at subcarrier index t1, t2, t3 and t4). The spectral shaping equation in terms of the above parameters is as follows

$$S(i \cdot \Delta f) \leq tss_i^2 \leq 1, \text{ for } 1 \leq i \leq 2 \times NSC - 1$$

where $S(f) = \sum_n S_b \left(f - n \cdot \left(\frac{N}{NSC} \right) \cdot f_s \right)$,

$$S_b(f) = \sum_{k \in SUPPORTEDset} tss_k^2 \times (W^2(f - k \cdot \Delta f) + W^2(f + k \cdot \Delta f))$$

(N/NSC) is the Inverse Discrete Fourier Transform (IDFT) oversampling factor, with N and NSC are the number of samples in time domain and subcarriers, respectively Δf is the subcarrier frequency spacing, i.e. = 4.3125 kHz, f_s is the sampling frequency, i.e. $2 \times NSC \times \Delta f$, $W^2(f)$ is the Fourier transform of the autocorrelation function of a rectangular window, define as: $W^2(f) = \frac{17}{16} \times \sin^2 \left(\frac{f}{\frac{16}{17} \cdot \Delta f} \right)$.

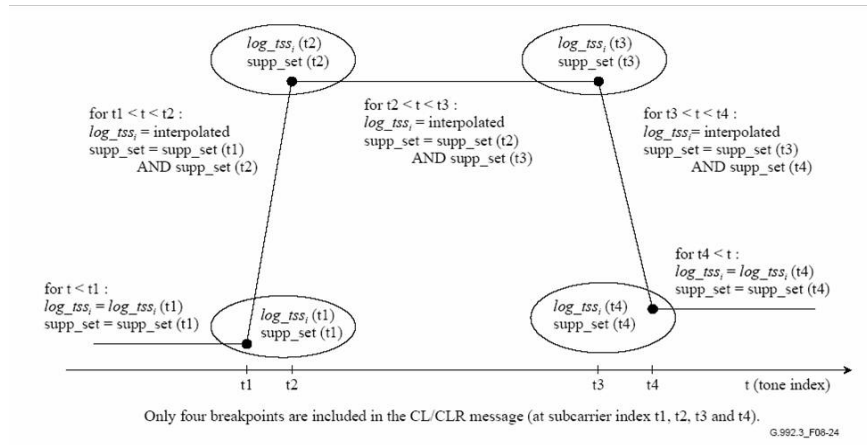


Figure 4: Illustration of the interpolation of \log_{tss_i} and indications.

One example of the downstream tss_i values as a function of the subcarrier index i , for the case that the SUPPORTEDset contains the subcarriers with index $i = 40$ to 200 and $N = 2 \times NSC = 512$ (oversampled IDFT). At frequencies $i \times \Delta f$, with $40 \leq i \leq 200$ and $\Delta f = 4.3125$ kHz, the tss_i value equals 1 (0 dB), is shown in Fig. 5. The blue curve indicates the spectral shaping in terms of tss_i shown as the red curve.

During the Channel Discovery Phase, the receive Physical Media Dependent (PMD) function may include the BLACKOUT bits (i.e., BLACKOUT_{*i*} for $i = 1$ to $NSC - 1$) in the MSG-PCB message. These contain a per subcarrier indication of whether the subcarrier may (BLACKOUT_{*i*} = 0) or may not (BLACKOUT_{*i*} = 1) be transmitted by the transmit PMD function during initialization. The MEDLEYset is defined as the set of subcarriers contained in the SUPPORTEDset, with removal of the subcarriers contained in the BLACKOUTset. ATU-R shall select a C-TREF pilot subcarrier from the MEDLEYset.

Application of spectral shaping and blackout during initialization is shown in Fig. 6. The values Z_i (for $i = 1$ to $2 \times NSC - 1$) are input to the modulation function.

1.5.3 Receiver-determined pilot tones

During initialization, the ATU-R receive PMD function selects the subcarrier index of the downstream pilot tone. Pilot tones only apply for downstream directions. They can be used for the timing recovery and reference

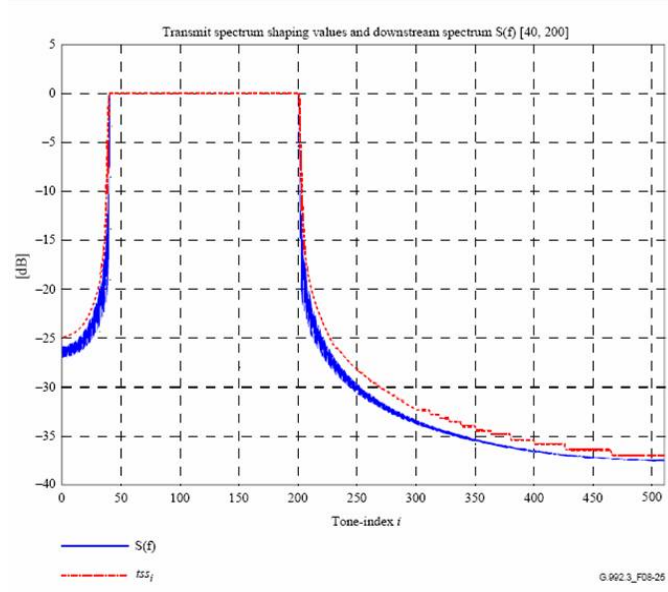


Figure 5: Example of the downstream $\log_{10} tss_i$ values in dB as a function of the subcarrier index.

Initialization phase	Spectrum shaping and subcarrier blackout application
G.994.1 (8.13.2)	No spectrum shaping and no blackout applied
Channel Discovery (8.13.3)	$Z_i = tss_i \times (X_i + jY_i)$ No blackout applied Nonzero $(X_i + jY_i)$ shall be scaled to the <i>NOMPSD</i> level
Transceiver Training (8.13.4)	$Z_i = tss_i \times (X_i + jY_i)$ if $BLACKOUT_i = 0$ $Z_i = 0$ if $BLACKOUT_i = 1$ Nonzero $(X_i + jY_i)$ shall be scaled to the <i>REFPSD</i> level
Channel Analysis (8.13.5)	$Z_i = tss_i \times (X_i + jY_i)$ if subcarrier in MEDLEYset $Z_i = 0$ if subcarrier not in MEDLEYset Nonzero $(X_i + jY_i)$ shall be scaled to the <i>REFPSD</i> level
Exchange (8.13.6)	$Z_i = tss_i \times (X_i + jY_i)$ if subcarrier in MEDLEYset $Z_i = 0$ if subcarrier not in MEDLEYset Nonzero $(X_i + jY_i)$ shall be scaled to the <i>REFPSD</i> level

Figure 6: Application of spectral shaping and blackout during initialization

and transmitted at REFPSD level as defined in 1.5.1.

R-MSG-FMT includes one bit parameter, FMT-C-PILOT which indicates whether the ATU-R requests the ATU-C to transmit a fixed 4-QAM constellation point on the C-TREF pilot tone. Set to 1 indicates it does. Set to 0 indicates it does not.

R-MSG-PCB includes one byte parameter, C-PILOT which is the sub-carrier index of downstream pilot tone chosen from the MEDLEYset.

1.6 On-line Reconfiguration

On-line reconfiguration [1, Ch. 10.2] allows the ADSL transceiver units (ATU) to autonomously maintain operation within limits set by control parameters. This is particularly useful when line or environment conditions are slowly changing, which is the case in ADSL deployments. When the control parameters cannot be maintained through autonomous on-line reconfiguration, an error condition occurs.

On-line reconfiguration is also used to optimize ATU settings following initialization, especially when using the fast initialization sequence that requires making faster estimates during training. In addition, higher layer data, management, and control functions can make use of on-line reconfiguration. In these cases, the on-line reconfiguration is associated with various application options of ADSL.

There are three types of on-line reconfiguration specified in the standard: Bit Swapping, Dynamic Rate Repartitioning, and Seamless Rate Adaptation. The three types are ordered in increasing degrees of freedom.

1.6.1 Bit Swapping

Bit Swapping (BS) reallocates data and power among the data subcarriers without modification of the higher layer features of the physical layer. Bit Swapping reconfigures the bits and fine gain parameters without changing any other higher layer control parameters. After a Bit Swapping reconfiguration, the total data rate ($\sum L_p$) is unchanged and that data rate on each latency path (L_p)¹ is also unchanged. Because bit swapping is used for autonomous changes to maintain the operating conditions for the modem during changing environment conditions, BS is a mandatory feature.

¹Latency paths are paths through the physical layer with different latency characteristics, which allows the support of varying applications that require different performance and robustness characteristics. ADSL2 supports up to 4 latency paths.

1.6.2 Dynamic Rate Repartitioning

Dynamic Rate Repartitioning (DRR) is used to reconfigure the data rate allocation between multiple latency paths (L_p). DRR can also include modifications to the bits and fine gain parameters, reallocating bits among the subcarriers, and is thus a superset of BS. DRR does not modify the total data rate ($\sum L_p$) but does modify the individual latency path data rates (L_p). Because DRR is used in response to higher layer commands, DRR is an application option. The ability to support DRR is identified during the initialization procedure.

1.6.3 Seamless Rate Adaptation

Seamless Rate Adaptation (SRA) is used to reconfigure the total data rate ($\sum L_p$) by modifying the frame multiplexer control parameters (L_p) and modifications to the bits and fine gains parameters. Since the total data rate is modified, at least one latency path (or more) will have a new data rate (L_p) after the SRA. SRA allows modulation parameters to change without modifying framing parameters. This prevents frame de-synchronization which causes uncorrectable bit error or system retraining. Since SRA is used in response to higher layer commands, SRA is an application option. The ability to support SRA is identified during the initialization procedure. Any ATU that implements the optional short initialization procedure should implement SRA operations. This ensures the ATU is able to adapt to the channel conditions which were not as accurately estimated because of the short training period.

1.6.4 On-line reconfiguration procedure

The following is a simplified on-line reconfiguration protocol:

1. RX monitors the SNR of channel and determines rate change is necessary
2. RX sends message to initiate rate change, which includes all necessary parameters, e.g. bits and gains info on each subchannel
3. TX sends SYNC FLAG signal used as a marker to designate exact time where the new parameters will be used
4. RX detects SYNC FLAG and both seamlessly and transparently transition to the data rate

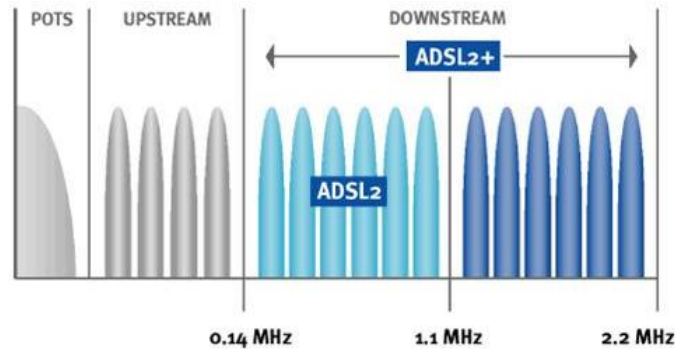


Figure 7: ADSL2+ doubles the downstream bandwidth compared to ADSL2 [3]

1.7 ADSL2+

ADSL2+ was ratified by the ITU in January 2003, joining the ADSL2 standards family as G.992.5 [2]. ADSL2+ doubles the transmission bandwidth, with all of the new bandwidth allocated to downstream channels, thereby increasing the downstream data rate for shorter copper lines (< 5000 feet). Since longer lines would experience more severe attenuation at the higher frequencies, increasing the downstream bandwidth by including higher frequencies does not increase the data rate for long lines.

While ADSL2 specifies a downstream frequency band up to 1.1 MHz, ADSL2+ specifies a downstream frequency band up to 2.2 MHz (see Fig. 7). This results in a significant increase in downstream data rates on shorter lines, as can be seen in Fig. 8.

2 Multichannel DMT

In this section, we discuss the potential improvements to the data rate performance in DMT systems when more than one line is used for data transmission. We call these techniques multichannel DMT methods. We focus on three different multichannel DMT methods: loop bonding (Sec. 2.1), spectrum balancing (Sec. 2.2), and vectored-DMT (Sec. 2.3). These methods are ordered in increasing levels of coordination required among the multiple transceivers.

Loop bonding is considered a static spectrum management method, since the spectral masks are determined up front and do not change over time. This is the method proposed in the ADSL2 standard to increase the data

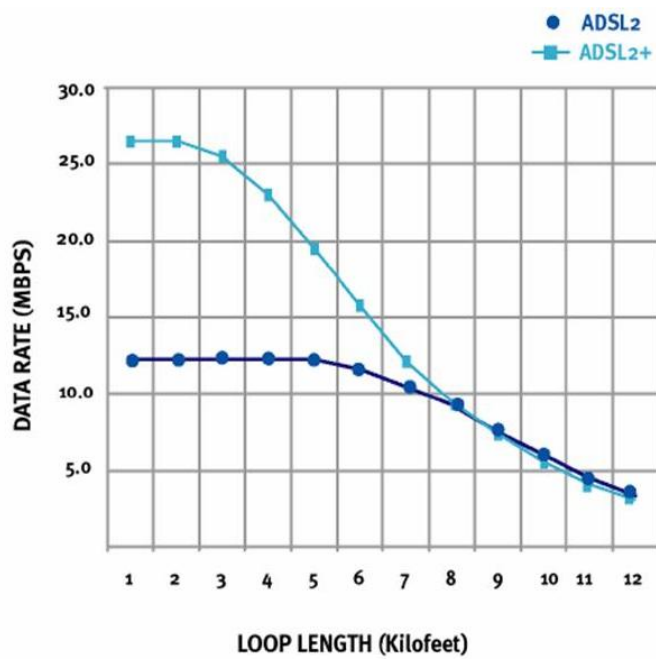


Figure 8: ADSL2+ approximately doubles the downstream data rates compared to ADSL2 for short (< 5 kilofeet) lines [3]

rates by using more than one copper line. A major disadvantage of using loop bonding is its inherent requirement of imposing strict spectral masks on the transmitted signals. This is because the design has to accommodate the worst case cross-talk levels, in order to prevent disastrous performance when these worst case levels are in fact realized. This overly conservative approach is unable to exploit the time-varying nature of the channel, which clearly would have better-than-the worst-case crosstalk levels almost all the time.

This is the main motivation for the spectrum balancing and vectored DMT methods, which are called dynamic spectrum management (DSM) methods [5]. DSM allows adaptive allocation of spectrum across the different lines by making the allocation a function of the physical channel characteristics at the current time instant. The allocation can then be performed such that certain performance measures are maximized. This allows a better utilization of the copper lines, and hence achieves higher data rates than static spectrum management.

We shall discuss two main forms of DSM: spectrum balancing (Sec. 2.2) and vectored-DMT (Sec. 2.3). In spectrum balancing, the allocation of spectra across tones and across the copper lines is determined from the direct and crosstalk channel characteristics, and thus allows efficient utilization of the channel. Vectored-DMT goes one step further by performing intelligent signal processing in order to remove the cross-talk altogether given the channel characteristics, hence achieving very high overall data rates.

In order for both DSM methods to work, accurate information about the direct channel characteristics and the crosstalk channel characteristics are required. This requires more elaborate channel identification methods, and is the subject of Section 2.4.

2.1 Loop Bonding

Loop bonding [3] is a method recommended in the ADSL2 standard to further increase the data rates by bonding multiple phone lines together [1, Ch. K.2]. This is supported in the ATM transmission convergence (ATM-TC) layer, through ATM Forum's inverse multiplexing for ATM (IMA) standard [6]. Through IMA, ADSL2 chipsets can bind two or more copper pairs in an ADSL link, and achieve data rates approximately twice that of using only one copper line (Fig. 9).

The IMA standard specifies a new sublayer that resides between the physical layer (PHY) and the ATM-TC layer. The transmitter takes in a single ATM stream from the ATM layer and distributes this stream, in a

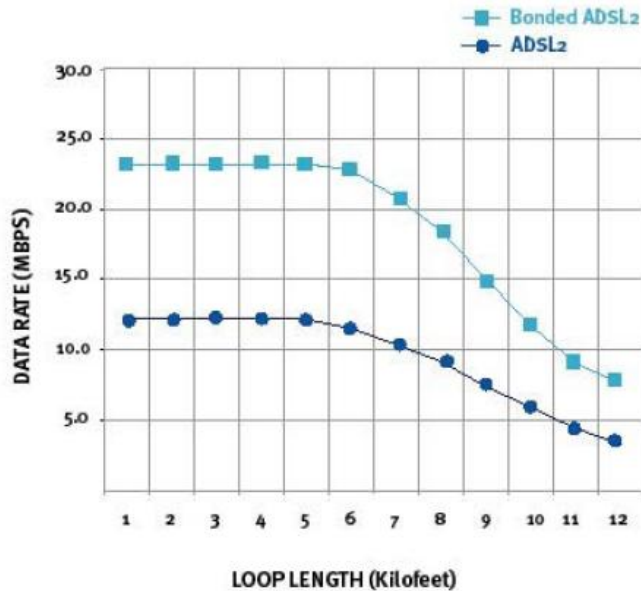


Figure 9: Loop bonding allows allows for multiplication of the data rate. [3]

round robin manner, to the multiple ADSL PHYs called an IMA group. At the receiver side, the IMA sublayer takes in the ATM cells and reconstructs the original stream. Figure 10 shows the basic functionality of IMA.

The IMA standard specifies the framing, protocols, and management functionality necessary when the PHYs are lossy, asynchronous, and have different delays. In order to work under these conditions, the IMA standard also requires modifications to some of the standard ADSL2 PHY functions. This include the discarding of idle cells [1, Ch. K.2.8.2] and errored cells [1, Ch. K.2.8.5] at the receiver.

In order to implement ADSL2 loop bonding using IMA, the ATM transmission convergence layer should be used. Some intellectual property vendors have IMA compliant cores for a field programmable gate array (FPGA), e.g. Xilinx [7]. This allows a service provider that uses ATM-TC to easily incorporate IMA functionality in existing ADSL2 deployments. If ATM is not the transport protocol used, IMA is clearly not directly applicable. However, IMA could still be used as a guide to implement a bonding solution for, e.g. TCP-IP based links.

One of the biggest advantages of using loop bonding is its inherent simplicity, i.e. very minimal changes to existing DMT transceivers are necessary, since coordination is performed at a higher layer. This assumes that

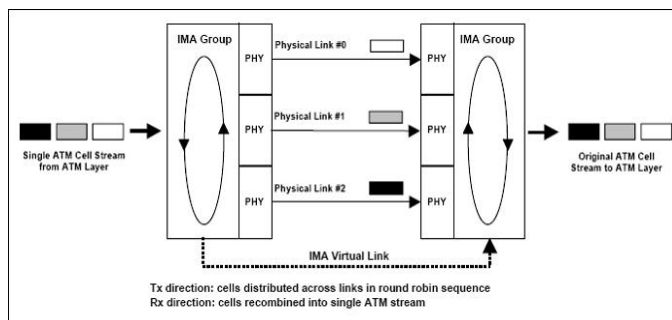


Figure 10: Basic IMA functionality for bonding three ADSL PHYs [6]

cross talk coupling among the lines is not a major issue. This is a reasonable assumption when strict spectral mask constraints are imposed on the DMT modems, which minimize the impact of crosstalk on the aggregate data rates.

2.2 Spectrum Balancing

Spectrum balancing methods decide the spectral assignment for each separate line, given their channel characteristics. There are two main themes in spectral assignment: margin adaptive and rate adaptive. In margin adaptive spectral assignment or power control, the objective is to minimize the amount of power allocated such that certain target rates are achieved. In rate adaptive spectral assignment or power control, the objective is to maximize the total data rate subject to power constraints. Note that these two themes are duals of each other, and hence solving one actually solves the other problem too.

It is well known that for the case of a single line, the optimal solution for both rate and power adaptive allocation is a 'water-filling' power spectral density [8]. We discuss the single-line water-filling solution for the margin-adaptive case in Sec. 2.2.1.

For multiple lines, performance evaluation and optimization become much more complex. We shall discuss two multiple-line spectrum balancing methods: distributed (Sec. 2.2.3) and centralized (Sec. 2.2.4) power control. Distributed power control does not require run-time coordination among the multiple lines, and allows the multiple receivers to execute the power control algorithm independently of the other receivers. Centralized power control, on the other hand, executes its algorithm at the transmitter end, after the channel characteristics of all the lines have been received.

2.2.1 Single-line Power Control

For the single-line margin-adaptive power control problem, we wish to find the set of power levels for each tone in the DMT symbol such that the total power required is minimized and a target overall data rate is achieved. Mathematically, this can be written as

$$\begin{aligned}
 P^* &= \min_{P_n} \sum_{n=1}^N P_n & (1) \\
 \text{s.t.} & \sum_{n=1}^N \log_2 \left(1 + \frac{P_n \gamma_n}{\Gamma} \right) = R
 \end{aligned}$$

where N is the number of tones in the DMT symbol, P_n is the power loaded into tone n , γ_n is the signal-to-noise ratio (SNR) on tone n , Γ is the SNR gap², and R is the target data rate. We also assumed that the rate for each tone n is given by $R_n = \log_2 \left(1 + \frac{P_n \gamma_n}{\Gamma} \right)$; which can take on a continuous set of non-negative real values.

In order to solve (1), we use the method of Lagrangian multipliers and solve the dual problem. We form the Lagrangian, and take its partial derivative with respect to P_n and set it to zero,

$$\begin{aligned}
 \frac{\partial L}{\partial P_n} &= \frac{\partial \left\{ \left(\sum_{n=1}^N P_n \right) + \lambda \left(\log_2 \left(1 + \frac{P_n \gamma_n}{\Gamma} \right) - R \right) \right\}}{\partial P_n} \\
 &= 1 + \frac{\lambda}{\ln(2)} \frac{1}{\left(\frac{\Gamma}{\gamma_n} + P_n \right)} = 0 \\
 \Rightarrow & \frac{\Gamma}{\gamma_n} + P_n = K, \quad n = 1, \dots, N
 \end{aligned}$$

where K is a constant value that needs to be found such that $\sum_{n=1}^N P_n = P_{total}$ and $P_n \geq 0$. This is the well known waterfilling result, which is depicted in Fig. 11.

Conceptually, we load more power to the tones with higher signal-to-noise ratio, and turn off tones below the 'waterlevel' K .

The previous formulation assumes that a continuum of rates is possible. In practice, we typically have a discrete set of rates available only, e.g. 1-15

²A constant value which depends on the modulation, coding, and margin desired, such that a certain bit error rate is achieved.

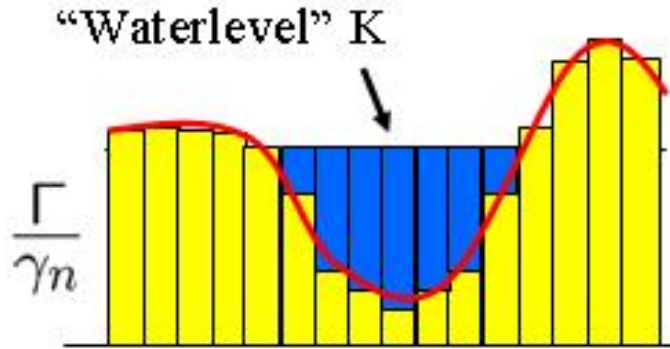


Figure 11: Waterfilling concept for optimal power control in DMT. The inverse of the signal-to-noise ratio is plotted for each tone. We pour 'water' (power) into the tones until the 'water-level' (K) is attained.

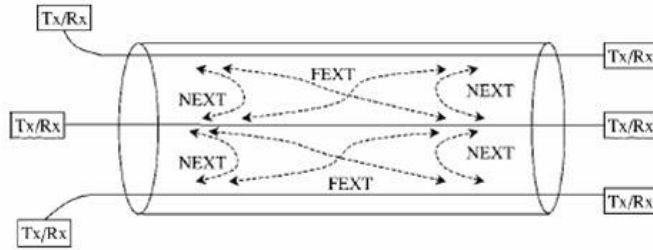


Figure 12: Crosstalk in a multi-line DMT system [9].

bits per subcarrier in ADSL2. Fortunately, an optimal greedy bit-loading algorithm is also available, which can be summarized conceptually as—*while the target rate is not yet achieved, find the tone which has not reached the maximum number of bits, and requires the least amount of power to increase by 1 bit, and load that amount of power to that tone.*

2.2.2 Multi-line Power Control

The cross-talk environment in a multiple line system is shown in Fig. 12. Because of the coupling among the lines, energy from nearby lines leak into the each other, and cause unnecessary interference. This interference can be modeled as additional noise contributing to the line of interest. The margin adaptive and rate adaptive power control problems are given by (2) and (3) respectively.

$$P^* = \min_{P_{k,n}} \sum_{k=1}^K \sum_{n=1}^N P_{k,n} \quad (2)$$

$$s.t. \quad \sum_{n=1}^N \log_2 \left(1 + \frac{P_{k,n} |H_{k,n}|^2}{\Gamma_k \left(\sigma_{k,n}^2 + \sum_{j \neq k} P_{j,n} |H_{j,n}|^2 \right)} \right) = R_k$$

$$R^* = \max_{P_{k,n}} \sum_{k=1}^K \sum_{n=1}^N \log_2 \left(1 + \frac{P_{k,n} |H_{k,n}|^2}{\Gamma_k \left(\sigma_{k,n}^2 + \sum_{j \neq k} P_{j,n} |H_{j,n}|^2 \right)} \right) \quad (3)$$

$$s.t. \quad \sum_{n=1}^N P_{k,n} \leq \bar{P}_k \\ P_{k,n} \geq 0, \quad \forall k, n$$

where $H_{k,n}$ and $\sigma_{k,n}^2$ are the complex channel gain and noise variance for line k on subcarrier n , respectively; and Γ_k and \bar{P}_k are the SNR gap and total power constraint for line k . These optimization problems are non-convex problems, and hence solving them is much more difficult than solving the convex single-line problem. In the following, we discuss two methods to solve this problem: iterative waterfilling, and optimal spectrum management.

2.2.3 Iterative Waterfilling

Iterative waterfilling [9] is an extension of the single-line waterfilling process for the multi-line case. This algorithm is based on formulating the power-allocation problem as a competitive game, in which each line tries to maximize his own data rate while regarding crosstalk interference from the other lines as noise. Starting from any initial spectra, the waterfilling procedure is performed independently across all the lines. It can be shown that this distributed iteration process converges to a competitively optimal equilibrium point. Furthermore, the convergence and uniqueness of an iterative waterfilling solution from any initial spectra are guaranteed for all DSL lines [9]. This iterative waterfilling procedure is illustrated in Fig. 13.

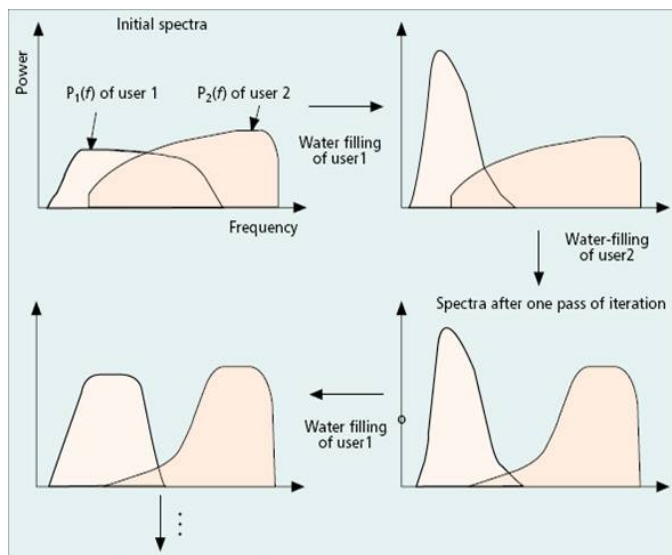


Figure 13: Iterative waterfilling spectra for two users after one iteration [10].

Notice the tendency of the power allocation spectra to move away from each other. The algorithm typically converges after a few iterations (≈ 3).

A simplified flowchart for rate-adaptive iterative waterfilling for two users is shown in Fig. 14. Assuming a common power constraint for the two users, waterfilling is performed independently for the two users to determine the power allocation P_i . If the resulting data rate R_i is greater than equal to the target data rate T_i , the power allocation P_i is decreased by a small constant value δ ; otherwise, it is increased by the same constant amount.

In order to truly implement the iterative waterfilling algorithm distributively, each receiver must know its target data rate *a priori*. It is important for the target data rates to be achievable, otherwise some receivers may operate with negative margins. This set of data rates can be determined off line during the loop planning stage.

2.2.4 Optimal spectrum management

The iterative waterfilling approach converges to a unique point, but it does not guarantee optimality. If coordination among the transmitters is possible, then the centralized optimal spectrum management (OSM) algorithm [11] can be used to achieve better performance than the previous method.

The OSM algorithm attempts to solve the rate-adaptive problem with

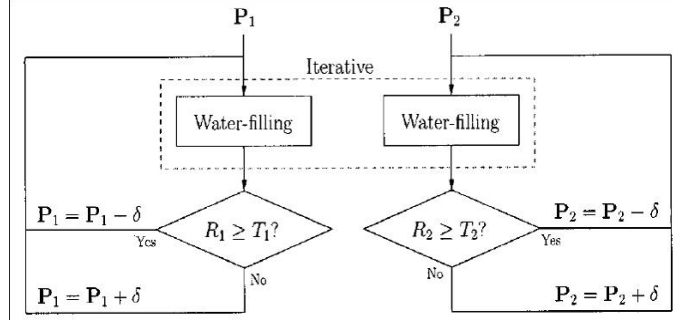


Figure 14: Simplified illustration of the iterative waterfilling algorithm for two users [9].

rate constraints, given as

$$\begin{aligned}
 R_K^* &= \max_{P_{k,n}} R_K & (4) \\
 \text{s.t.} & R_k \geq T_k, \quad k = 1, \dots, K-1 \\
 & \sum_{n=1}^N P_{k,n} \leq \bar{P}_k, \quad \forall k \\
 & P_{k,n} \geq 0, \quad \forall k, n
 \end{aligned}$$

where $R_k = \sum_{n=1}^N r_{k,n}$ is the rate for line k , with $r_{k,n} = \log_2 \left(1 + \frac{P_{k,n}|H_{k,n}|^2}{\Gamma_k \left(\sigma_{k,n}^2 + \sum_{j \neq k} P_{j,n}|H_{j,n}|^2 \right)} \right)$

as the rate for each subcarrier n for line k , and where Γ_k and T_k are the SNR gap and target data rate for user k .

An equivalent weighted rate-sum formulation is used to solve (4), given as

$$\begin{aligned}
 R^* &= \max_{P_{k,n}} \sum_{k=1}^K w_k R_k & (5) \\
 \text{s.t.} & \sum_{n=1}^N P_{k,n} \leq \bar{P}_k, \quad \forall k \\
 & P_{k,n} \geq 0, \quad \forall k, n
 \end{aligned}$$

where w_k is a weight assigned to line k , such that $\sum_{k=1}^K w_k = 1$.

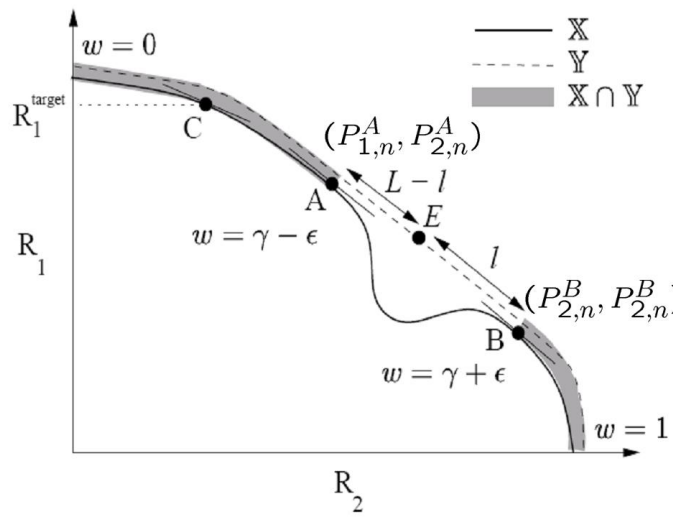


Figure 15: Graphical example of DSL systems having a close to convex rate region [11].

Any achievable point on the boundary of the convex hull of the rate region can be found through this maximization. Thus, if the rate region is close to being convex, then majority of the optimal operating points can be found. If the number of tones is large, and the channel gain of nearby tones are approximately the same, then the rate region is close to convex. This can be seen in Fig 15. Suppose that the tone spacing is fine enough such that M adjacent tones have approximately the same direct and crosstalk channel responses. Consider two points in the rate region for a two-user system, $A = (R_1^A, R_2^A)$ and $B = (R_2^B, R_2^B)$ and their corresponding power spectral densities (PSD) $(\mathbf{P}_1^A, \mathbf{P}_2^A)$ and $(\mathbf{P}_1^B, \mathbf{P}_2^B)$. It is possible to operate at a point $E = (\frac{m}{M}R_1^A + \frac{M-m}{M}R_1^B, \frac{m}{M}R_2^A + \frac{M-m}{M}R_2^B)$ for any $0 \leq m \leq M - 1$. This is done by setting the PSD to $(\mathbf{P}_1^A, \mathbf{P}_2^A)$ on tones $n \in \{pM + 1, \dots, pM + m\}$ for all integers p such that $pM + m \leq N$, and to $(\mathbf{P}_1^B, \mathbf{P}_2^B)$ on all other tones. Thus, if M is large, almost every point on the convex hull of the rate region can be achieved. Fortunately, this is the case for most practical DSL systems, thus solving the weighted rate-sum problem in (4) solves the original problem in (5).

In order to solve the original problem given by (4), a dual optimization approach using Lagrangian multipliers can be used. Consider the Lagrangian,

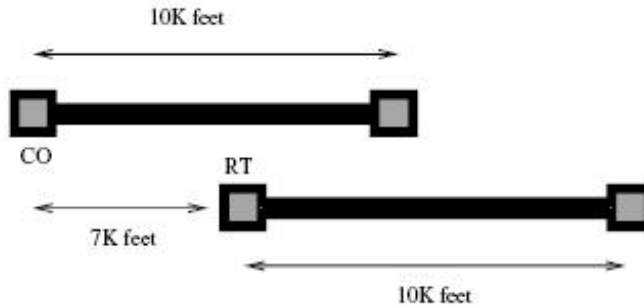


Figure 16: Two-user ADSL scenario used for the comparison [12].

$$\begin{aligned}
 L &= \sum_{k=1}^K w_k R_k + \sum_{k=1}^K \lambda_k \left(\bar{P}_k - \sum_{n=1}^N P_{k,n} \right) \\
 &= \sum_{k=1}^K \sum_{n=1}^N w_k r_{k,n} - \sum_{k=1}^K \sum_{n=1}^N \lambda_k P_{k,n} + \sum_{k=1}^K \lambda_k \bar{P}_k \\
 &= \sum_{n=1}^N L_n(w_k, \lambda_k) + \sum_{k=1}^K \lambda_k \bar{P}_k
 \end{aligned}$$

where $L_n(w_k, \lambda_k) = \sum_{k=1}^K (w_k r_{k,n} - \lambda_k P_{k,n})$. This can be considered as N per-tone optimizations coupled only through w_k and λ_k . Thus, the complexity is linear in the number of tones N , but still exponential in the number of lines K , where $K \ll N$. This is because an exhaustive search of all possible combinations of w_k and λ_k is still required for each tone. This is a huge complexity reduction, since solving the original problem directly would be exponential in N . Lower complexity approaches that avoids the exhaustive search has also been proposed in [12].

A comparison among the various approaches is shown for the two-user ADSL scenario (Fig. 16) in Fig. 17. It can be seen from this scenario that OSM achieves higher rates than iterative waterfilling, and the lower complexity OSM search comes quite close to the OSM rates.

2.3 Vectored-DMT

The spectrum balancing approaches described in Sec. 2.2 use power control to make the most use of the direct and crosstalk channel characteristics.

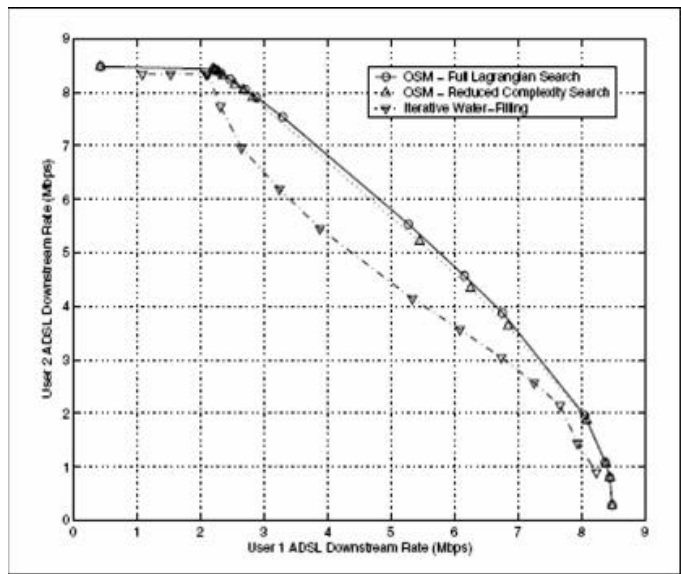


Figure 17: Comparison of rate regions among the three different approaches: iterative waterfilling (Sec. 2.2.3), optimal spectrum management (OSM) with exhaustive search proposed in [11], and OSM using low complexity search proposed in [12]. (Figure from [12].)

The vectored-DMT approach [13] goes one step further by treating the multi-channel DMT channel as a multiple-input multiple-output (MIMO) channel, and uses signal processing techniques to cancel out the crosstalk altogether. In order for this approach to be viable, block transmission and reception at the central office has to be synchronized, and an accurate estimate of the MIMO channel matrix must also be available.

2.3.1 Upstream: Successive interference cancelation

Consider the received signal vector \mathbf{z}_i for tone i given as

$$\mathbf{z}_i = \mathbf{T}_{i,\text{up}}\mathbf{u}_i + \mathbf{n}_i, \quad i = 1, \dots, N \quad (6)$$

where $\mathbf{T}_{i,\text{up}}$ is the $K \times K$ MIMO uplink channel matrix for tone i , whose diagonal elements are the direct channel complex gains, and the off-diagonal elements are the crosstalk complex channel gains; and where \mathbf{u}_i and \mathbf{n}_i are the transmitted symbol vector, and uncorrelated noise vector for tone i respectively.

Consider performing a QR factorization (see e.g. [14]) of the MIMO channel matrix in (6), $\mathbf{T}_{i,\text{up}} = \mathbf{Q}_{i,\text{up}}\mathbf{R}_{i,\text{up}}$, where $\mathbf{Q}_{i,\text{up}}$ is a unitary matrix, and $\mathbf{R}_{i,\text{up}}$ is an upper triangular matrix. Multiplying the received signal vector \mathbf{z}_i with the Hermitian conjugate of $\mathbf{Q}_{i,\text{up}}$, we have

$$\begin{aligned} \tilde{\mathbf{z}}_i &= \mathbf{Q}_{i,\text{up}}^* \mathbf{z}_i \\ &= \mathbf{Q}_{i,\text{up}}^* (\mathbf{Q}_{i,\text{up}} \mathbf{R}_{i,\text{up}} \mathbf{u}_i + \mathbf{n}_i) \\ &= \mathbf{R}_{i,\text{up}} \mathbf{u}_i + \tilde{\mathbf{n}}_i \end{aligned}$$

where $\tilde{\mathbf{n}}_i = \mathbf{Q}_{i,\text{up}}^* \mathbf{n}_i$ has an identity covariance matrix, because $\mathbf{Q}_{i,\text{up}}$ is unitary. Since $\mathbf{R}_{i,\text{up}}$ is upper triangular and $\tilde{\mathbf{n}}_i$ has uncorrelated components, the input symbol vector \mathbf{u}_i can be recovered by back-substitution combined with symbol-by-symbol detection. The detection of the k th element of \mathbf{u}_i can be expressed as

$$(\hat{\mathbf{u}}_i)_k = \text{decode} \left[\frac{1}{r_{k,k}^i} (\tilde{\mathbf{z}}_i)_k - \sum_{j=k+1}^K \frac{r_{k,j}^i}{r_{k,k}^i} (\hat{\mathbf{u}}_i)_j \right]; \quad k = K, K-1, \dots, 1$$

where $r_{k,j}^i$ is the (k, j) th element of $\mathbf{R}_{i,\text{up}}$. Assuming that the previous decisions are correct, crosstalk is completely canceled, and L parallel channels are created within each tone.

2.3.2 Downstream: MIMO Precoding

For downstream transmission, consider the QR decomposition of the transpose of the downstream MIMO channel, given as

$$\mathbf{T}_{i,\text{dn}}^T = \mathbf{Q}_{i,\text{dn}} \mathbf{R}_{i,\text{dn}} \quad (7)$$

By transmitting $\mathbf{u}_i = \mathbf{Q}_{i,\text{dn}}^{T*} \mathbf{R}_{i,\text{dn}}^{-T} \text{diag}(\mathbf{R}_{i,\text{dn}}^T) \tilde{\mathbf{u}}_i$, and after being multiplied by the channel $\mathbf{T}_{i,\text{dn}}$, the received signal is given by

$$\begin{aligned} \mathbf{z}_i &= \mathbf{R}_{i,\text{dn}}^T \mathbf{Q}_{i,\text{dn}}^T \mathbf{u}_i \\ &= \mathbf{R}_{i,\text{dn}}^T \mathbf{Q}_{i,\text{dn}}^T \mathbf{Q}_{i,\text{dn}}^{T*} \mathbf{R}_{i,\text{dn}}^{-T} \text{diag}(\mathbf{R}_{i,\text{dn}}^T) \tilde{\mathbf{u}}_i \\ &= \text{diag}(\mathbf{R}_{i,\text{dn}}^T) \tilde{\mathbf{u}}_i \end{aligned}$$

which is a cross-talk free signal. Tomlinson-Harashima precoding (see [15] and [16]) can also be used to prevent unwanted energy increase.

2.4 Initialization

2.4.1 Training Sequences

A known training sequence can be transmitted to estimate the channel impulse response before data transmission in a digital communication system. Training sequences are either periodic or aperiodic [17]. In either case, the power spectrum of the training sequence is approximately flat over the transmission bandwidth. The suggested training sequence for channel estimation in a DMT system is a pseudo-random binary sequence with M samples [1]. The training sequence is made periodic by repeating M samples or by adding a cyclic prefix. The training sequence design could be based on a time domain or frequency domain. A time-domain design method is introduced in [18]. A disadvantage of the time-domain method is that an exhaustive search for the optimal training sequence of length M requires $2M$ possible sequences. A frequency-domain method is proposed to reduce the computational cost in [19]. However, the frequency-domain method cannot always find the optimal periodic training sequence in terms of the mean-squared channel estimation error [18]. A summary and comparison for these design methods is shown in the table. A training sequence is said to be perfect or optimal in the table if it have impulse-like autocorrelation and zero cross-correlation [20]. N is the length of a training sequence in the table. So, the design is a tradeoff between the searching complexity and the sequence performance.

Table 2: Comparison of training sequence design methods

Domain	Method	Minimum MSE	Searching Complexity	Optimal Sequence
Time	Periodic[18]	Yes	High(2^N)	Yes
Time	Aperiodic [17]	No	Medium(N^2)	Yes
Time	L-Perfect (MIMO)[20]	Almost	Low($N\log_2 N$)	Sometimes
Frequency	Periodic [19]	No	Low($N\log_2 N$)	Sometimes

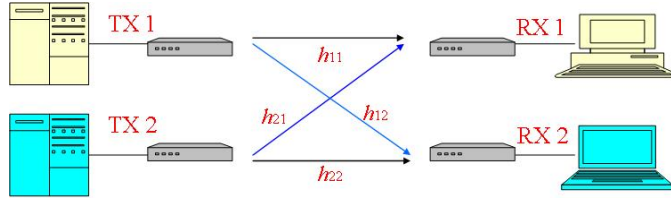


Figure 18: 2×2 MIMO Channel Model

2.4.2 Channel Model

Consider a system that employs two-transmit and two-receive antennas simply. Two training signals and are transmitted over four wired channels $\mathbf{h}_{ij}(L) = [h_{ij}(0) \cdots h_{ij}(L-1)]^T$, i or $j = 1, 2$ where $(\cdot)^T$ denotes the transpose operation. L denotes the maximum number of channel taps. \mathbf{h}_{11} and \mathbf{h}_{22} are main direct channel impulse responses between the same transmitter and receiver. \mathbf{h}_{21} and \mathbf{h}_{12} are cross channel impulse responses between the different transmitter and receiver. Each channel is modeled as a finite-impulse response (FIR) filter with L taps. The input training sequences \mathbf{s}_1 and \mathbf{s}_2 belong to a finite-signal constellation and are transmitted in data blocks where each block consists of N_i information symbols and N_t training symbols. For two transmitters, the receiver uses the $2N_i$ known training symbols to estimate the unknown $2L$ channel coefficients. The observed training sequence output that does not have interference from information or preamble symbols can be expressed as

$$\mathbf{y} = \begin{bmatrix} \mathbf{y}_1 \\ \mathbf{y}_2 \end{bmatrix} = \mathbf{S}\mathbf{h} + \mathbf{z} = \begin{bmatrix} \mathbf{S}_1(L, N_t) & \mathbf{S}_2(L, N_t) \end{bmatrix} \begin{bmatrix} \mathbf{h}_{11}(L) & \mathbf{h}_{12}(L) \\ \mathbf{h}_{21}(L) & \mathbf{h}_{22}(L) \end{bmatrix} + \mathbf{z} \quad (8)$$

where \mathbf{y} and \mathbf{z} are of dimension $2(N_t - L + 1) \times 1$, \mathbf{z} is assumed to be additive white Gaussian noise(AWGN). \mathbf{S}_1 and \mathbf{S}_2 are Toeplitz matrices of dimension

Table 3: Comparison among multichannel DMT techniques

	Loop Bonding (Sec. 2.1)	Iterative Waterfilling (Sec. 2.2.3)	Optimal Spectrum Management (Sec. 2.2.4)	Vectored-DMT (Sec. 2.3)
Design Complexity	Low	Medium	Medium	High
Computational Complexity	Low	Medium	Very High	High
Level of Coordination	Low	Medium	High	Very High
Data-rate Performance	Low	Medium	High	Very High

$(N_t - L + 1) \times L$, and

$$\mathbf{S}_i(L, N_t) = \begin{bmatrix} s_i(L-1) & \cdots & s_i(0) \\ s_i(L) & \cdots & s_i(1) \\ \vdots & \ddots & \vdots \\ s_i(N_t-1) & \cdots & s_i(N_t-L) \end{bmatrix}, i = 1, 2$$

3 Preliminary Design Recommendations

In this section, we present preliminary design recommendations for the downlink of a multichannel DMT system, where the transmitter has limited computational complexity. We first present the multichannel DMT technique tradeoffs, and the recommended methods to be used under certain scenario in Sec. 3.1. We then present the recommended training and channel estimation methods for the MIMO channel in Sec. 3.2.

3.1 Multichannel Technique Recommendations

The choice of the most appropriate multichannel technique is a computational complexity and achievable data-rate tradeoff. This can be summarized in Table 3.

If the channel has limited cross-talk coupling, or, if the data rates achievable when strict spectral masks are imposed to limit cross-talk is good enough, then loop bonding is the best choice for its low design and computational complexity, and its low required level of coordination.

If a limited redesign is tolerable, iterative waterfilling is a good method to employ to increase the data rates achievable, since the algorithm can easily be added into the receivers without requiring coordination among them. OSM is the next method of choice if higher data rates are desired, but this is at the expense of a high computational complexity. If block synchronization at the receivers is not a problem, vectored-DMT has lower complexity, and could potentially achieve higher data rates than OSM. The upstream method of successive interference cancelation is the preferred method, since this relieves the burden from the transmitters, and lets the receivers perform the burden of increased synchronization and computational complexity.

3.2 Initialization Recommendations

We wish to determine a training sequence which optimized the mean-squared estimation error for a least-squares type channel estimator. According to the model shown as above, a simple and intuitive method to estimate the MIMO channel impulse responses h_{11} , h_{22} , h_{12} and h_{21} , is to send the training sequence \mathbf{s} at only one transmitter by turning off another transmitter during one training time slot.

This method has very low complexity and does not require design of a special training sequence. However, training time is longer, since it needs two time slots to obtain the estimated channels. During the first time slot,

$$h_{11} = \frac{y_{t_1,1}}{s}, h_{12} = \frac{y_{t_1,2}}{s}$$

and for the second time slot,

$$h_{21} = \frac{y_{t_2,1}}{s}, h_{22} = \frac{y_{t_2,2}}{s}$$

However, traditionally, the linear least square channel estimates can be calculated as [21]

$$\hat{\mathbf{h}} = \begin{bmatrix} \hat{h}_{11} & \hat{h}_{12} \\ \hat{h}_{21} & \hat{h}_{22} \end{bmatrix} = (\mathbf{S}^H \mathbf{S})^{-1} \mathbf{S}^H \mathbf{y}$$

where $(\cdot)^H$ and $(\cdot)^{-1}$ denote the complex-conjugate (Hermitian) transpose and the inverse, respectively. The mean-squared error (MSE) for the time-domain case is defined by

$$\text{MSE} = E \left[(\mathbf{h} - \hat{\mathbf{h}})^H (\mathbf{h} - \hat{\mathbf{h}}) \right] = 2\sigma^2 \text{Tr}((\mathbf{S}^H \mathbf{S})^{-1})$$

where we assume white noise with auto-correlation matrix $\mathbf{R}_z = E [zz^H] = 2\sigma^2 \mathbf{I}_{N_t-L+1}$, \mathbf{I}_n denotes the identity matrix of dimension $n \times n$, and $\text{Tr}(\cdot)$

denotes the trace of a matrix. The minimum mean-squared error (MMSE) is equal to

$$\text{MMSE} = \frac{2\sigma^2 L}{N_t - L + 1}, \text{ iff } \mathbf{S}^H \mathbf{S} = \begin{bmatrix} \mathbf{S}_1^H \mathbf{S}_1 & \mathbf{S}_2^H \mathbf{S}_1 \\ \mathbf{S}_1^H \mathbf{S}_2 & \mathbf{S}_2^H \mathbf{S}_2 \end{bmatrix} = (N_t - L + 1) \mathbf{I}_{2L} \quad (9)$$

The training sequences \mathbf{s}_1 and \mathbf{s}_2 that satisfy (5) are considered as optimal sequences. So, (9) tells us that the optimal sequences have an impulse-like auto-correlation sequence and zero cross correlation.

A simple method to design two optimal training sequences \mathbf{s}_1 and \mathbf{s}_2 of length N_t to estimate two channels each of L taps, is to design instead a single training sequence of length $N_t + L + 1$ to estimate a single channel with $2L$ taps. \mathbf{s}_1 and \mathbf{s}_2 could be constructed as

$$\mathbf{s}_1 = [s(0) \dots s(N_t)], \mathbf{s}_2 = [s(L) \dots s(N_t + L)]$$

But it has the high searching complexity though it can obtain the MMSE.

Another method is to transmit the two same consecutive training sequences \mathbf{s}_1 at each transmitter, $[\mathbf{S}_1 \quad -\tilde{\mathbf{S}}_1^*]$ at one transmitter and $[\mathbf{S}_1 \quad \tilde{\mathbf{S}}_1^*]$ at another transmitter. The operation denoted by $\tilde{(\cdot)}$ refers to time-reversing a sequence. The $(\cdot)^*$ denotes the complex conjugate of the sequences. The received signals during two time slots can be expressed as

$$\begin{bmatrix} \mathbf{y}_1 \\ \mathbf{y}_2 \end{bmatrix} = \underbrace{\begin{bmatrix} -\tilde{\mathbf{S}}_1^* & \tilde{\mathbf{S}}_1^* \\ \mathbf{S}_1 & \mathbf{S}_1 \end{bmatrix}}_{\mathbf{S}} \begin{bmatrix} \mathbf{h}_{11}(L) & \mathbf{h}_{12}(L) \\ \mathbf{h}_{21}(L) & \mathbf{h}_{22}(L) \end{bmatrix} + \mathbf{z}$$

If the sequence \mathbf{s}_1 is symmetric about its center with impulse-like auto correlation, I can get $\mathbf{S}^H \mathbf{S} = (N_t - L + 1) \mathbf{I}_{2L}$ which is the condition to achieve the MMSE and optimal sequence in (9).

References

- [1] *Asymmetric digital subscriber line (ADSL) transceivers 2*, ITU-T Std. G.992.3, 2002.
- [2] *Asymmetric digital subscriber line (ADSL) transceivers 2 - Extended bandwidth ADSL2 (ADSL2+)*, ITU-T Std. G.992.5, 2003.
- [3] "ADSL2 and ADSL2plus-The New ADSL Standards," 2003. [Online]. Available: http://www.dslforum.org/aboutdsl/ADSL2_wp.pdf

- [4] L. F. Wei, "Trellis-coded modulation with multidimensional constellations," *IEEE Trans. Inform. Theory*, vol. 33, pp. 483–501, July 1987.
- [5] J. Cioffi. Dynamic spectrum management project. [Online]. Available: <http://www-isl.stanford.edu/cioffi/dsm/>
- [6] *Inverse Multiplexing for ATM (IMA)*, ATM Forum Std. af-phy-0086.001, Mar. 1999. [Online]. Available: <ftp://ftp.atmforum.com/pub/approved-specs/af-phy-0086.001.pdf>
- [7] "Inverse Multiplexing for ATM (IMA) Solutions with Spartan-II FPGAs," 2000. [Online]. Available: <http://www.xilinx.com/bvdocs/whitepapers/wp107.pdf>
- [8] T. M. Cover and J. A. Thomas, *Elements of information theory*. New York: Wiley, 1991.
- [9] W. Yu, G. Ginis, and J. Cioffi, "Distributed Multiuser Power Control for Digital Subscriber Lines," *IEEE J. Select. Areas Commun.*, vol. 20, no. 5, pp. 1105–1115, June 2002.
- [10] K. B. Song, S. T. Chung, G. Ginis, and J. Cioffi, "Dynamic spectrum management for next-generation DSL systems," *IEEE Commun. Mag.*, vol. 40, no. 10, pp. 101–109, 2002.
- [11] R. Cendrillon, W. Yu, M. Moonen, J. Verlinden, and T. Bostoen, "Optimal Multi-user Spectrum Management for Digital Subscriber Lines," *IEEE Trans. Commun.*, to appear.
- [12] W. Yu, R. Lui, and R. Cendrillon, "Dual optimization methods for multiuser orthogonal frequency division multiplex systems," in *Proc. IEEE Global Telecommunications Conference*, vol. 1, Dec. 2004, pp. 225–229.
- [13] G. Ginis and J. Cioffi, "Vectored Transmission for Digital Subscriber Line Systems," *IEEE J. Select. Areas Commun.*, vol. 20, no. 5, pp. 1085–1104, June 2002.
- [14] D. S. Watkins, *Fundamentals of Matrix Computations*, 2nd ed. New York: John Wiley, 2002.
- [15] M. Tomlinson, "New automatic equalizer employing modulo arithmetic," *Electronic Letters*, vol. 7, pp. 138–139, Mar. 1971.

- [16] H. Harashima and H. Miyakawa, "Matched-transmission technique for channels with intersymbol interference," *IEEE Trans. Commun.*, vol. COM-20, pp. 774–780, Aug. 1972.
- [17] C. Tellambura, Y. J. Guo, and S. K. Barton, "Channel estimation using aperiodic binary sequence," *IEEE Commun. Lett.*, vol. 2, pp. 140–142, May 1998.
- [18] W. Chen and U. Mitra, "Frequency domain versus time domain based training sequence optimization." *Proc. IEEE Int. Conf. Comm*, June 2000, pp. 646–650.
- [19] C. Tellambura, M. G. Parker, Y. Guo, S. . Shepherd, and S. . K. Barton, "Optimal sequences for channel estimation using discrete fourier transform techniques," *IEEE Transactions on Communications*, vol. 47, no. 2, pp. 230–238, Feb. 1999.
- [20] C. Fragouli, N. Al-Dhahir, and W. Turin, "Training-based channel estimation for multiple-antenna broadband transmissions," *IEEE Transactions on Wireless Communications*, vol. 2, no. 2, pp. 384–391, March 2003.
- [21] T. Kailath, A. H. Sayed, and B. Hassibi, *Linear Estimation*. Englewood Cliffs, NJ: Prentice-Hall, 2000.